Earth and Planetary Science Letters 584 (2022) 117513

Contents lists available at ScienceDirect

Earth and Planetary Science Letters

www.elsevier.com/locate/epsl

The essential bioactive role of nickel in the oceans: Evidence from nickel isotopes

Nolwenn Lemaitre *, Jianghui Du, Gregory F. de Souza, Corey Archer, Derek Vance

Department of Earth Sciences, Institute of Geochemistry and Petrology, ETH Zürich, Zürich, Switzerland

ARTICLE INFO

Article history:
Received 23 December 2021
Received in revised form 16 March 2022
Accepted 20 March 2022
Available online xxxx
Editor: L. Coogan

Keywords:
nickel isotopes
phytoplankton requirement
bio-availability
GEOTRACES

ABSTRACT

The role of nickel (Ni) in ocean biogeochemical cycles is both under-studied and controversial. Strong correlations between Ni and organic carbon in modern and ancient marine sediments suggest a prominent biogeochemical role over a substantial portion of Earth history. Addition of Ni to culturing and seawater incubation experiments produces strong responses in terms of cell growth, particularly of nitrogen-fixing organisms. But the implied limiting role for phytoplankton growth is inconsistent with observations in the real ocean, specifically that photic zone Ni concentrations never descend to the very low values that characterise other bioactive, and often bio-limiting, metals like iron. These two observations can be reconciled if a large portion of the total dissolved Ni present in open-ocean surface waters is not bio-available on short timescales. Here we present new Ni concentration and stable isotope data from the GEOVIDE transect in the North Atlantic. We interpret these new data in the light of the growing database for Ni stable isotopes in the modern ocean, with implications for the biogeochemical importance of Ni.

In the new North Atlantic dataset, the lowest Ni concentrations (1.8-2.6 nmol/L) and highest δ^{60}Ni (up to +1.67‰) are associated with low nitrate, south of the subarctic front (SAF). By contrast, stations at latitudes north of the SAF, with higher surface nitrate, show very subdued variation in Ni concentrations throughout the entire depth of the water column (3.6±0.3 nmol/L, mean and 2SD), and no variation in δ^{60}Ni beyond the narrow global deep-ocean range (+1.33±0.13 ‰). These North Atlantic Ni isotope data also show relationships with nitrogen isotope effects, observed in the same samples, that are suggestive of a link between Ni utilisation, isotope fractionation and nitrogen fixation.

The global dataset, including the new data presented here, reveals a biogeochemical divide with Ni isotope fractionation only occurring in low latitude surface waters. A simple observationally constrained three-dimensional model of Ni cycling suggests that the creation of this isotopically heavy, Ni-poor, end-member, together with the physical circulation and remineralisation at depth, can explain the global Ni-δ^{60}Ni systematics. Taken together, these findings hint at Ni-N co-limitation in the modern ocean. We advocate for more extensive and detailed culturing/incubation studies of this neglected metal in order to elucidate its potentially crucial biogeochemical role.

1. Introduction

Nickel (Ni) is a bioactive metal that has garnered less scientific attention than many other transition metals, although it plays a key role in eight different enzyme systems (Ragsdale, 2009). The terminal step in methanogenesis involves methyl-coenzyme reductase (MCR), containing the Ni cofactor F_{430} and, in fact, three of the known Ni enzymes are found in methanogens (Watt and Ludden, 1999). The idea that methanogenesis is one of the most ancient metabolisms on Earth has led to the suggestion that the surface Earth abundance of Ni may have controlled atmospheric chemistry on the early Earth (e.g., Konhauser et al., 2009). The long-term importance of Ni to the oceanic biosphere is highlighted by its very prominent sedimentary association with organic carbon (Algeo and Maynard, 2004; Böning et al., 2015; Ciscato et al., 2018).

In the modern ocean, the most relevant Ni-bearing enzymes are those associated with nitrogen acquisition and fixation (e.g., urease, Ni-superoxide dismutase, Ni-Fe hydrogenases; Ragsdale, 2009). The nutrient-like distribution of Ni in the dissolved pool of the modern ocean, specifically drawdown in the photic zone and high concentrations at depth, is consistent with these biological roles (Sclater et al., 1976; Bruland, 1980; Mackey et al., 2002; Wang

* Corresponding author.
E-mail address: nolwenn.lemaitre@erdw.ethz.ch (N. Lemaitre).

https://doi.org/10.1016/j.epsl.2022.117513

et al., 2019; Archer et al., 2020; Middag et al., 2020; Yang et al., 2021). However, the nutrient-like distribution of Ni is characterised by an intriguing and unique feature. In contrast to the major nutrients, and to bioactive metals such as iron, zinc and cadmium (Bruland et al., 2014), photic zone Ni concentrations are never drawn down to very low levels (Sclater et al., 1976; Bruland, 1980; Mackey et al., 2002; Wang et al., 2019; Archer et al., 2020; Middag et al., 2020; Yang et al., 2021). While this could simply suggest that Ni is never a limiting nutrient, a number of studies have speculated that the residual photic zone concentrations of about 1.7-1.8 nmol/L may not be bio-available (e.g., Mackey et al., 2002; Archer et al., 2020; Middag et al., 2020).

Results from controlled culturing experiments provide support for this latter view, and have led to different conclusions regarding the importance of Ni for oceanic primary producers, and specifically whether the availability of this metal could be limiting to phytoplankton growth (Price and Morel, 1991; Dupont et al., 2008a, 2010; Egleston and Morel, 2008; Ho, 2013). Laboratory-cultured diatoms show a strong growth response to additions of Ni when grown on urea as the sole nitrogen (N) source (Price and Morel, 1991; Egleston and Morel, 2008), consistent with the role of Ni as a co-factor in urease, the enzyme that phytoplankton employ to recycle urea to ammonia. The same studies find that Ni is not drawn down when diatoms are instead grown on nitrate or ammonia. In contrast to (eukaryotic) diatoms, (prokaryotic) cyanobacteria respond strongly to Ni additions regardless of the nitrogen source, due to their additional requirement for the Ni form of the enzyme superoxide dismutase (SOD). This enzyme, of which there are several metallomic forms (Cu/Zn-, Fe-, Mn-, Ni-SOD), is essential for catalysing the breakdown of the toxic superoxide radicals generated by photosynthesis (Ragsdale, 2009). The Ni-SOD isoform is the only one found in all *Prochlorococcus*, in most *Synechococcus* and in some heterotrophic bacteria strains (Dupont et al., 2008a, 2008b). Interestingly, insufficient Ni supply has been shown to limit the growth and the nitrogen fixation rate of *Trichodesmium*, a cyanobacterial diazotroph (Ho, 2013; Ho et al., 2013; Rodriguez and Ho, 2014).

Recently, the stable isotope system of Ni has begun to be harnessed to address these questions, and the ocean biogeochemistry of Ni more generally. Thus far, the deep open ocean is characterised by a relatively homogeneous Ni isotope composition (δ^{60}Ni = variations in ^{60}Ni/^{58}Ni expressed in parts per thousand deviation from the NIST SRM986 standard), despite a three-fold variation in Ni concentrations (δ^{60}Ni = +1.33 ± 0.13‰ for depths >500 m, n = 135, mean and 2SD; Cameron and Vance, 2014; Takano et al., 2017; Wang et al., 2019; Archer et al., 2020; Yang et al., 2020, 2021), though with a suggestion of a small isotopic difference between the Pacific and Atlantic basins (Yang et al., 2021). Upwelling waters in the Southern Ocean are homogeneous in δ^{60}Ni over the entire water column, and show only a slight decrease in concentration at the surface (e.g., Cameron and Vance, 2014; Wang et al., 2019). However, the low latitude surface ocean, where Ni concentrations decrease to levels close to the 1.7-1.8 nmol/L minimum, show higher δ^{60}Ni, suggesting a significant fractionation associated with biological uptake. It is currently unclear whether the marine isotope systematics of Ni require this residual photic zone Ni to be in a form that is not bio-available (Archer et al., 2020; Yang et al., 2021).

Here, we have two main objectives. Firstly, we present new data for the water column of the North Atlantic Ocean, on samples obtained during the GEOVIDE (GEOTRACES GA01) cruise in 2014. Significantly for the above discussion, this cruise represents a transect across contrasting oceanic regimes, including the oligotrophic lower latitudes as well as more productive higher latitude waters (Fig. 1). We couple the new Ni-δ^{60}Ni data with available constraints from the same samples on nitrogen cycling. Secondly, we go beyond this specific new dataset and compile the growing global ocean Ni isotope database to suggest that there is a distinctive biogeochemical divide between the low and high latitude regimes, and that this divide has its origin in different phytoplankton ecologies with contrasting nitrogen cycling. Using a simple three-dimensional Ni cycling model, we show that global Ni-δ^{60}Ni systematics can be explained by enhanced low-latitude Ni utilisation and associated loss of isotopically light Ni from the low-latitude surface ocean. We provide further hints that the low latitude regime may see significant Ni-N co-limitation, suggesting a much more important biogeochemical role for Ni in large parts of the global ocean than heretofore envisaged.

2. Materials and methods

2.1. Study area and sample collection

During the GEOVIDE cruise (15 May-30 June 2014; R/V *Pourquoi Pas?*), samples for dissolved Ni concentrations and isotope compositions were collected at 6 stations and 17 depths. These six stations are separated by the Subarctic Front (SAF; Fig. 1). Cold nutrient-rich and productive upper-ocean waters are found north of the SAF, at stations 32, 38, 44 and 69. In contrast, at lower latitudes, the upper ocean at stations 13 and 21 is characterised by warm, salty and oligotrophic waters, accompanied by lower chlorophyll-a concentrations (Moore et al., 2013). Another striking difference between these two physical-biogeochemical regions pertains to the main phytoplankton classes. Diatoms are generally limited by silicate south of the SAF and are also co-limited by nitrogen closer to the Iberian margin. Such low nutrient concentrations make picophytoplankton such as cyanobacteria more competitive because of their high surface-to-volume ratio (Fig. 1; Raven, 1998; Tonnard, 2018). Phosphate data are not available for GEOVIDE, but Fonseca-Batista et al. (2019), using climatological phosphate excess ($P^* = [PO_4^{3-}] - [NO_3^-]/16$; from World Ocean Atlas 2018; Garcia et al., 2019), indicate that high P* in surface waters sustains N_2 fixation at station 13. At station 21, there is no clear phosphate excess and the authors suggest that N_2 fixation may be sustained by the direct use of dissolved organic phosphorus (DOP) by diazotrophs.

For all stations, samples were collected using a clean rosette equipped with cleaned 12 L GO-FLO bottles, following the recommendations of the GEOTRACES cookbook (Cutter et al., 2017). The rosette was deployed on a 14 mm Kevlar cable with a dedicated, custom-designed clean winch. Immediately after recovery, the GO-FLO bottles were individually covered at each end with plastic bags to minimise contamination. Bottles were then transferred into a clean container (Class-100) for sampling. Seawater samples were filtered through 0.45 µm polyethersulfone filters (Pall, Supor^{TM}) mounted in Swinnex polypropylene filter holders (Millipore). Note that 0.02 µm, 0.2 µm and 0.45 µm filters have all been used for studies of dissolved Ni isotopes and other metals in the past (Cameron and Vance, 2014; Takano et al., 2017; Wang et al., 2019; Archer et al., 2020; Yang et al., 2020, 2021), with no differences between measured isotope ratios of the filtrate. Between 1 and 4 L of filtrate was collected in acid-cleaned polyethylene bottles. More details of the sampling procedure can be found in Gourain et al. (2019).

2.2. Analytical methods for Ni isotopes

The methods used here for Ni isotope analysis have been described in detail previously (Vance et al., 2016; Wang et al., 2019; Archer et al., 2020; Sun et al., 2021) and only a summary is given here. Briefly, a ^{61}Ni-^{62}Ni double-spike was added to all pH∼2 acidified samples and left to equilibrate for 48 hours. Samples

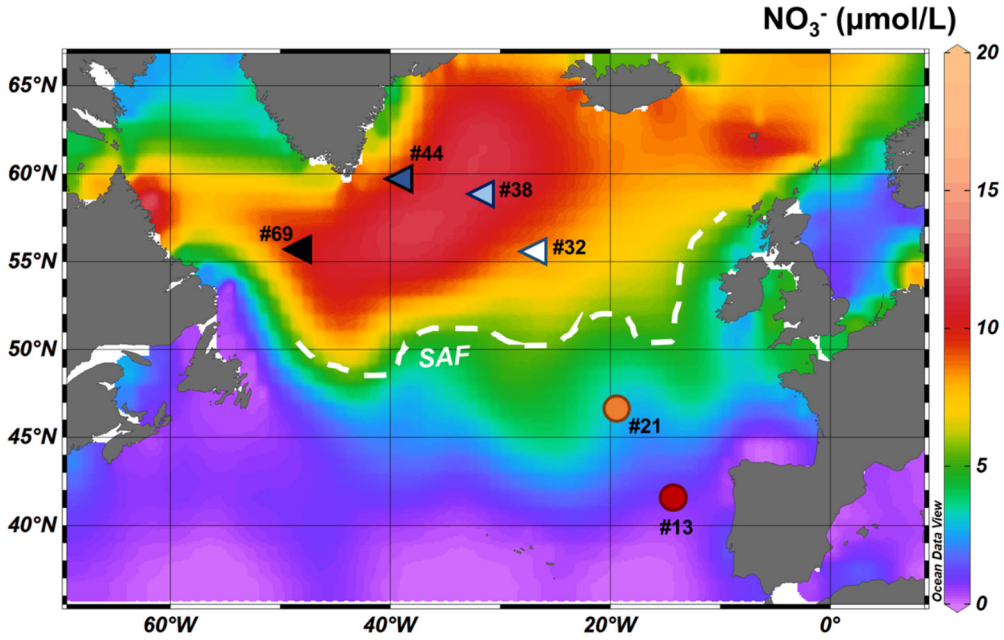

Fig. 1. Location of the sampling stations during the GEOVIDE cruise, superimposed on a map of the seasonal average nitrate (NO_3^-) concentrations at 5 m (April to June for the period 1955-2017; World Ocean Atlas 2018; Garcia et al., 2019). The approximate position of the subarctic front (SAF) is shown by the white dashed line (Zunino et al., 2017). The circle and triangle symbols correspond to the low and high latitude stations, respectively. (For interpretation of the colours in the figure(s), the reader is referred to the web version of this article.)

were then adjusted to pH 5.0 ± 0.3 using an ammonium acetate buffer, before loading onto the pre-concentration column. Ni was pre-concentrated from up to 2 L of seawater using an ethylenediaminetriacetic acid chelating resin, available commercially as Nobias PA-1 (Hitachi Technologies; Sohrin et al., 2008), to extract the trace metal inventory from the seawater matrix. To separate individual transition metals from each other and from the matrix, the pre-concentrated samples were passed through an anion-exchange column (Bio-Rad AG MP-1M resin). This produces an impure Ni fraction – for example, any residual Na or Mg not removed during the Nobias pre-concentration step would reside in this fraction. The impure Ni fraction was further purified by a second, much smaller Nobias resin column. Finally, this pure Ni was passed through a further small anion column (to remove any residual Zn and Fe).

Isotope analyses were performed using a Thermo-Scientific NeptunePlus multi-collector inductively-coupled-plasma mass spectrometer (MC-ICP-MS) at ETH Zurich. Nickel solutions were introduced into the mass spectrometer in 2% (v/v) (~0.3 mol/L) nitric acid via a CPI PFA nebuliser (50 µL/min) attached to a Cetac Aridus II desolvating nebuliser system. ^{56}Fe and ^{57}Fe were measured to monitor potential interference from ^{58}Fe on ^{58}Ni. These measured interferences were negligible. Mass discrimination was corrected using the double spike, as detailed previously (Cameron and Vance, 2014). All isotope compositions are given in standard delta notation as follows, relative to the NIST SRM 986 Ni standard:

$$\delta^{60}\mathrm{Ni}(‰) = \left[\frac{(^{60}\mathrm{Ni}/^{58}\mathrm{Ni})_{\mathrm{sample}}}{(^{60}\mathrm{Ni}/^{58}\mathrm{Ni})_{\mathrm{NIST\ SRM986}}} - 1\right] \times 1000$$

Concentrations of Ni were obtained using the isotope dilution approach from the double-spike data. Procedural blanks were determined for the same chemical separation protocol as for samples (i.e. acidified to pH~2, double-spiked and passed through the column chromatographic procedure), using 1L of ultra-pure Milli-Q water (>18.2 MΩ.cm) as the "sample". These procedural blanks were consistently determined to be <0.4 ng for Ni, and are therefore negligible.

Long-term reproducibility of isotope analyses was ±0.07‰ for Ni (2SD). This was assessed over the course of this and parallel studies, through repeat measurements of primary NIST and secondary (USGS Fe-Mn nodule, Nod-P1, digested and passed through the Ni column chemistry) standards for Ni. The USGS nodule gave $\delta^{60}Ni_{\mathrm{NIST\ SRM986}} = +0.35 \pm 0.07‰$ (2SD, n = 260 over 15 months). This is identical to values previously published: $\delta^{60}Ni_{\mathrm{NIST\ SRM986}} = +0.36 \pm 0.07‰$ (Gueguen et al., 2013). Internal errors obtained from the mass spectrometric analysis and propagated through the mass discrimination correction were generally lower than long-term reproducibility. These internal errors are given in Table S1. Uncertainties plotted on the figures are the internal uncertainties or the long-term reproducibility, whichever is the larger. Full duplicate analyses were carried out for 14 GEOVIDE samples. Results were consistent with long-term standard reproducibility, with differences between these replicates ranging from 0.05 to 0.16‰ (mean value 0.10±0.07‰, ±2SD, n=14). Our GEOVIDE Ni concentration and isotope data have been approved by the GEOTRACES Standards and Intercalibration (S&I) Committee and have been released in the GEOTRACES IDP2021 (GEOTRACES Intermediate Data Product Group, 2021).

2.3. Modelling global Ni cycling

Both ocean circulation and biological cycling control the oceanic distributions of Ni and its isotopes. Here we use a simple Ni cycling model to study these effects. The Supplementary Information provides full details of the model – here we give a summary. The model we use is the Total Matrix Intercomparison (TMI) (Gebbie and Huybers, 2010), which is conceptually similar to the Optimal Multi-Parameter Analysis (OMPA) for water mass decomposition (Karstensen and Tomczak, 1998). Unlike OMPA, TMI is a global water mass decomposition that avoids subjective definitions of ocean interior water mass end-members by tracing the ocean interior waters back to their surface origins (Gebbie and Huybers, 2010). The TMI solution is constrained by observational climatologies of hydrographic and biogeochemical parameters as described by Gebbie and Huybers (2010).

We first model the distribution of Ni and its isotopes only in terms of ocean circulation, where the concentrations of Ni in the ocean are modelled by propagating their surface boundary conditions using a circulation pathway matrix. The resulting fields represent the preformed component of the dissolved pool. We derive these surface boundary condition using the surface (<100 m) Ni concentration data of the GEOTRACES IDP2021 (GEOTRACES Intermediate Data Product Group, 2021). In the high latitude surface regions, including the Antarctic and Subantarctic Zones of the Southern Ocean, subpolar North Atlantic, subpolar North Pacific and Arctic, we use the data-based average Ni concentrations for the boundary condition. In the surface low latitude regions (~40°S to ~40°N; see Gebbie and Huybers, 2010), we take the boundary condition to be 2 nmol/L, which is the concentration found in these regions (Archer et al., 2020; Takano et al., 2017; Yang et al., 2021, 2020). The uncertainties on the boundary conditions of Ni concentration are propagated through the model (Fig. S1).

We then calculate the isotopic surface boundary condition using published data (Fig. S2) for surface waters in high latitudes (δ^{60}Ni = +1.33‰; Cameron and Vance, 2014; Wang et al., 2019), and the value of ~ +1.7‰ that low latitude surface waters converge to (Archer et al., 2020; Takano et al., 2017; Yang et al., 2021, 2020). In the model we assume the uncertainty of the surface δ^{60}Ni boundary condition is ±0.07‰ (2σ) which is our analytical error. This error is then propagated through the model (Fig. S1).

We cannot explicitly model surface Ni biological cycling because TMI treats the surface as a boundary condition. However, we add an interior biological cycling term by linking Ni remineralisation to that of PO_4^{3-} and by linking remineralised phosphate to O_2. In the high latitudes, we assign a value of 0.52 mmol/mol to the regenerated Ni/PO_4 ratio ($r_{Ni/PO4}$), based on the Ni quota in diatoms. In the low latitudes, we assign a value of 3.4 mmol/mol to $r_{Ni/PO4}$ based on the Ni quota in cyanobacteria (Twining et al., 2012). We assume that there is no Ni isotope fractionation in the high latitude surface ocean, given the uniform surface and deep ocean δ^{60}Ni of ~ +1.33‰ in these regions (Cameron and Vance, 2014; Wang et al., 2019). The same δ^{60}Ni value is assigned to the regenerated pool derived from low latitude export. The offset to high δ^{60}Ni in low-latitude surface waters (+1.7‰) implies an isotope fractionation in the low latitude regions, which can be attributed either to uptake, or to an offset between the bioavailable and non-available pools. Observational constraints on the isotope composition of the low-latitude regenerated Ni come from two sources. The particulate data in Yang et al. (2021), which may contain more than purely biogenic material that would shift them towards lower δ^{60}Ni, show a maximum value of +1.2‰. Nickel in marine sediments, corrected for detrital Ni contributions, are identical to the deep ocean δ^{60}Ni at about +1.3‰. These small variations in regenerated δ^{60}Ni have a limited impact on our model, assessed through a sensitivity experiment in Fig. S3.

3. Results

The new GEOVIDE Ni concentrations and isotope compositions are presented in Fig. 2 and, together with macronutrient concentrations, in Table S1. Dissolved Ni concentrations vary from 1.75 to 5.68 nmol/L and exhibit lower concentrations at the surface compared to the deep ocean. However, this nutrient-like profile is very different in character north and south of the SAF (Fig. 2a and c). For the two stations south of the SAF (stations 13 and 21), Ni concentrations descend to 1.75 nmol/L in the upper 50 m. At these two stations, deep Ni concentrations are also the highest in the dataset (up to 5.7 nmol/L at depths around 4000 m), due to the high preformed concentrations of the southern-sourced lower North East Atlantic Deep Water ($NEADW_L$, also named Lower Deep Water; Dickson and Brown, 1994; García-Ibáñez et al., 2018). In contrast, the four stations north of the SAF do not show such strong surface−deep differences. In particular, surface Ni concentrations at these higher latitudes (3.45 ± 0.34 nmol/L in the upper 50 m of stations 32, 38, 44 and 69; mean ± 2SD) are very similar to those in deeper waters (3.68±0.20 nmol/L at depths >500 m; Fig. 2c). Ratios of lithogenic-corrected Ni to phosphorus (litho-corr pNi/pP) (Lemaitre et al., 2020) in photic zone particulates also differ between high and low latitudes. Higher ratios are observed south of the SAF (Fig. S4), perhaps indicating greater relative Ni uptake there compared to stations at higher latitude.

The Ni isotope composition is rather invariant in the deep North Atlantic (>500 m), averaging 1.36 ± 0.13‰, including in $NEADW_L$. This value is identical to the global average of +1.33 ± 0.13‰ (mean and 2SD >500 m, shaded band in Fig. 2; Cameron and Vance, 2014; Takano et al., 2017; Wang et al., 2019; Archer et al., 2020; Yang et al., 2020, 2021). But the Ni isotope composition in the upper ocean again exhibits distinctive behaviour depending on latitude. At high latitudes and north of the SAF (stations 32, 38, 44 and 69), the small decrease in Ni concentrations upwards into the photic zone is coupled to Ni isotopes that barely change over the entire water column (triangles in Fig. 2c and d). Conversely, the prominent drop in surface Ni concentrations at low latitude stations 13 and 21 is accompanied by significantly higher δ^{60}Ni, reaching up to +1.67‰ for concentrations of about ~2 nmol/L at the surface (circles in Fig. 2a and b). Similar contrasts between geographic regions have been observed in the literature (Cameron and Vance, 2014; Takano et al., 2017; Wang et al., 2019; Archer et al., 2020; Yang et al., 2020, 2021).

Our TMI model aims to assess the extent to which the first-order controls of biological cycling and ocean circulation can explain the marine Ni and δ^{60}Ni distributions. Model results generally reproduce the structure of the observations (Fig. 2; Figs. S1, S5). However, the model underestimates Ni concentrations in the deep Pacific, and along the GEOVIDE transect at depths of 100–400 m and 4000–4500 m in low latitude waters (Fig. 2a). These data-model differences could be the result of simplifications in the model, including the lack of a seasonal cycle, imperfect representation of the true circulation, limitation of modelled processes to physical circulation, uptake, remineralisation and the isotopically heavy surface end-member in low latitude waters and the simplicity of our biological parameterization. Alternatively, the mis-match may point to additional processes not included in the model and that should be investigated in the future, such as the possibility of a benthic source of Ni from sediments (Little et al., 2020; Gueguen and Rouxel, 2021).

4. Discussion

4.1. Nickel isotope fractionation linked to nitrogen fixation in the North Atlantic

The North Atlantic is characterised by strong spatial variability in fixed nitrogen (N) concentrations, with lower nitrate availability in the low latitude region (Fig. 1). Surface productivity in the North Atlantic subtropical gyre can be limited by nitrate (NO_3^-; Moore et al., 2013), where N_2 fixation performed by diazotrophs is the major source of bioavailable inorganic N in surface waters (Capone et al., 2005). Stable nitrogen and oxygen isotopes in NO_3^-, also determined during GEOVIDE, are used to determine Δ(15-18), which is defined as the difference between δ^{15}N and δ^{18}O of NO_3^- (Deman et al., 2021). Decoupling between nitrogen and oxygen isotopes in NO_3^-, reflected by a change in Δ(15-18), reflects nitrogen-cycling processes other than uptake or denitrification (for which Δ(15-18) is set to +3‰). In Fig. 3, low Δ(15-18) values are observed in both the low and high latitude regions. At high latitude stations, the

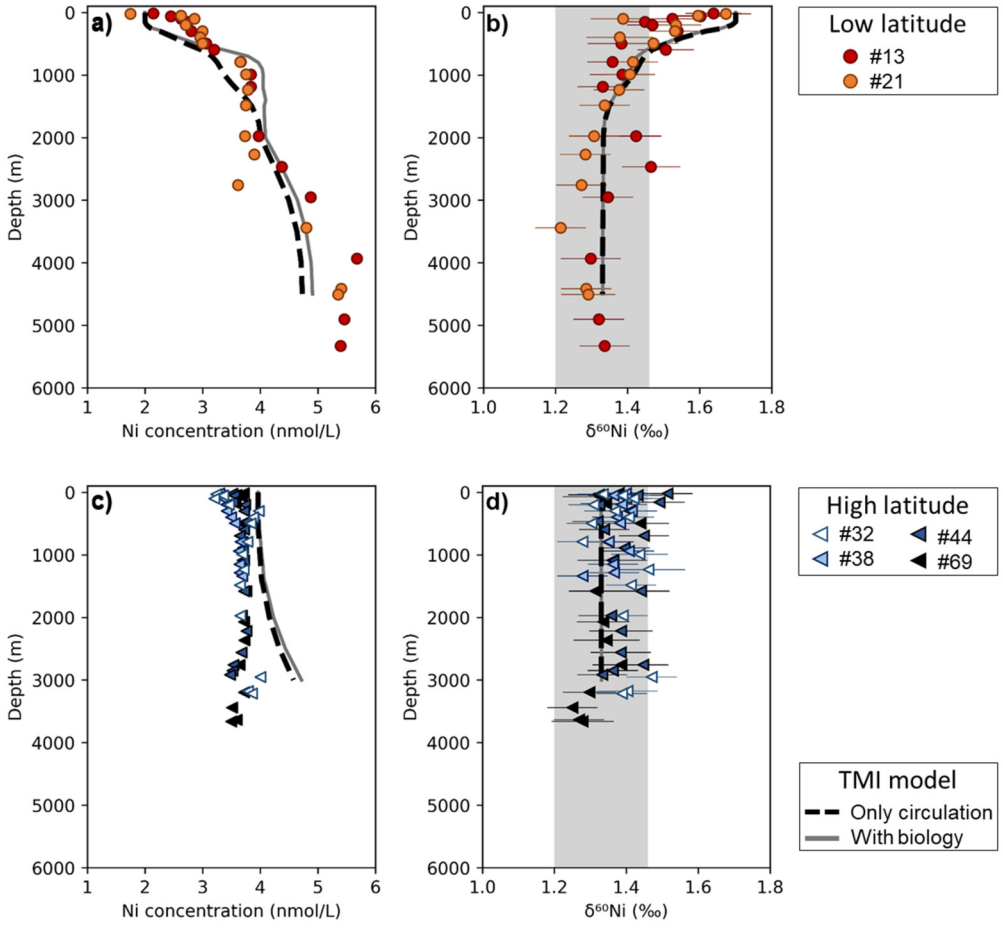

Fig. 2. Depth profiles of dissolved Ni concentrations and isotope compositions (δ^{60}Ni) at the six stations along the GEOVIDE transect. The top panels show data from the low latitude North Atlantic (Fig. 2a and b, south of the subarctic front; stations 13 and 21) and the bottom panels show the data from the high latitude North Atlantic (Fig. 2c and d, north of the subarctic front; stations 32, 38, 44, 69). The shaded grey band shows the average δ^{60}Ni in the deep ocean (1.33 ± 0.13‰, 2SD). Modelled Ni concentrations and δ^{60}Ni values obtained in the vicinity of station 21 (top panel) and station 69 (bottom panel) are also shown by a dashed black line (propagation of surface signals only) or a grey line (circulation and interior remineralisation). (For interpretation of the colours in the figure(s), the reader is referred to the web version of this article.)

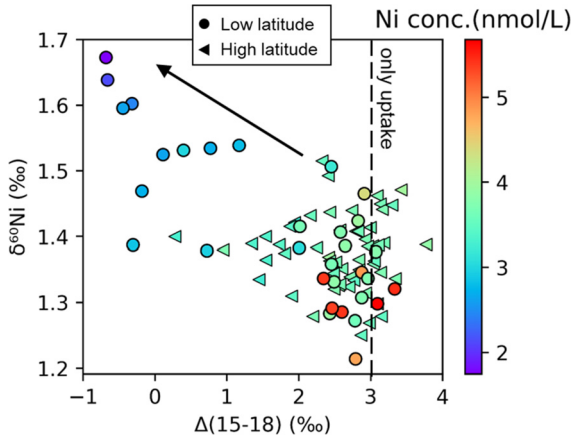

Fig. 3. Fractionation of Ni and NO_3^- isotopes. δ^{60}Ni plotted against Δ(15-18) (see Section 4.1 for definition), colour-coded for Ni concentrations, for data from the low (circles) and high (triangles) latitude stations of the GEOVIDE transect. (For interpretation of the colours in the figure(s), the reader is referred to the web version of this article.)

low values (down to +0.3‰) are due to an increase in δ^{18}O following remineralisation (Deman et al., 2021) and are accompanied by an average δ^{60}Ni value of +1.38‰, similar to the deep ocean signature. In contrast, the low Δ(15-18) values at the low latitude stations 13 and 21 (as low as −0.7‰) are accompanied by heavier Ni isotopes (Fig. 3), especially in the surface waters, where Ni concentrations are at their lowest. The decrease in Δ(15-18) from high to low latitudes results from a decrease in low-latitude δ^{15}N due to N_2 fixation (Deman et al., 2021). Following these authors, this δ^{15}N decrease likely results both from remote N_2 fixation in the broader North Atlantic subtropics and from local diazotrophy, as suggested by the significant N_2 fixation rates measured at low-latitude stations during GEOVIDE (Fonseca-Batista et al., 2019).

The association of low Ni concentrations and high δ^{60}Ni with low Δ(15-18) in surface and thermocline waters of the low latitudes suggests that N_2 fixation decreases δ^{15}N and elevates δ^{60}Ni in the low-latitude North Atlantic. Greater Ni uptake by nitrogen fixers has been demonstrated or suggested by many previous studies (Dupont et al., 2008a; Twining et al., 2012; Ho, 2013; Ho et al., 2013; Rodriguez and Ho, 2014; Middag et al., 2020). Takano et al. (2017) first reported surface Ni isotope fractionation in low latitude regions. Archer et al. (2020) confirmed this observation with a larger dataset, and noted that the high-low latitude difference in surface Ni isotope behaviour was associated with dramatic changes in water column ratios of Ni to major nutrients. These authors suggested a control on surface low latitude Ni isotope compositions via nitrogen-fixing cyanobacteria, a conclusion subsequently supported by Yang et al. (2020). In addition to the relationship between Ni and NO_3^- isotopes, the link between N_2 fixation and fractionation of Ni isotopes is strengthened by the covariation between a limited number of co-analysed N_2 fixation rates and δ^{60}Ni in surface waters (Fig. 4a). In Fig. 4b, the limited

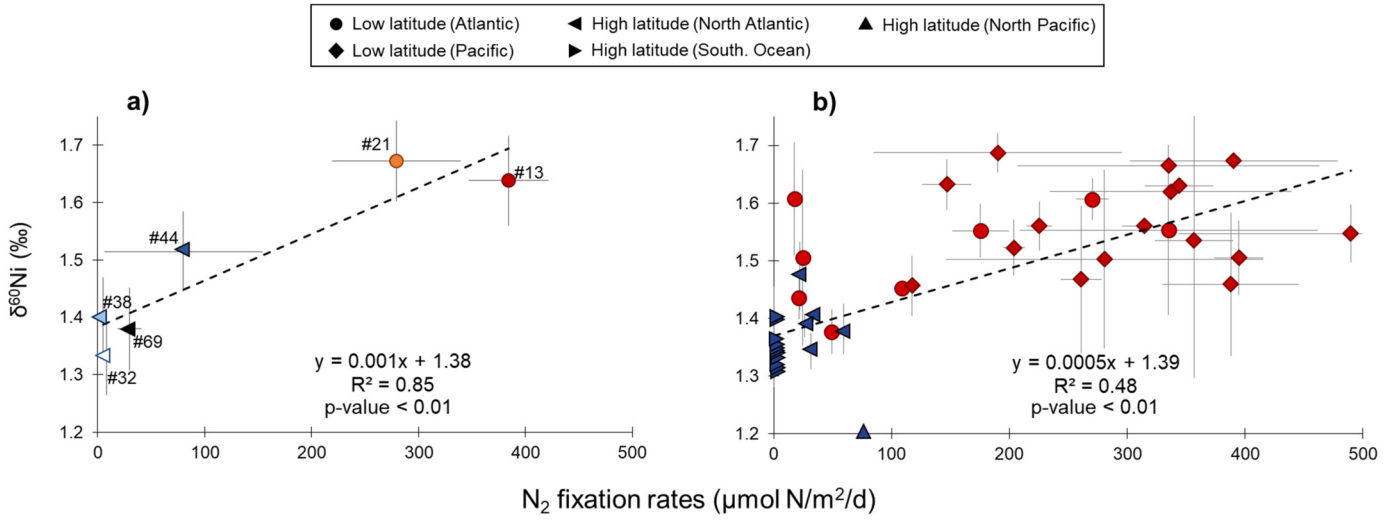

Fig. 4. Relationship between Ni isotopes and N_2 fixation rates **a)** for GEOVIDE stations with uppermost (15-30 m) Ni isotope compositions plotted versus euphotic layer-integrated (from the surface to 0.2% irradiance) N_2 fixation rates. **b)** for the world ocean with Ni isotope composition averaged in the upper 100 m (Cameron and Vance, 2014; Takano et al., 2017; Wang et al., 2019; Archer et al., 2020; Yang et al., 2020, 2021; this study) plotted versus N_2 fixation rates integrated in the upper 100 m and estimated by the DARWIN biogeochemical model (https://dataverse.harvard.edu/dataverse/GUD_CS510). Low latitude stations are shown in red and stations from high latitudes are in blue. (For interpretation of the colours in the figure(s), the reader is referred to the web version of this article.)

surface data are supplemented by modelled N_2 fixation rates at locations where surface δ^{60}Ni data are available (see Fig. S2) to show that such covariation exists on much broader spatial scales. High modelled N_2 fixation rates in the low latitude ocean are confirmed by other studies (Luo et al., 2012; Bonnet et al., 2017; Caffin et al., 2018; Fonseca-Batista et al., 2019; Selden et al., 2019; Tang et al., 2019; Gradoville et al., 2020). The causality of such covariations would, however, require confirmation via culture/incubation experiments.

In the oceanic photic zone, N_2 fixation is believed to be mostly performed by cyanobacteria (Capone et al., 2005). Phytoplankton pigment distributions along the GEOVIDE transect indicate that cyanobacteria are most abundant south of the SAF, especially in the Iberian basin (~20% of phytoplankton abundance at Station 13; Tonnard, 2018), where the highest N_2 fixation rates were measured (384 µmol N/m^2/d; Fonseca-Batista et al., 2019) and where a heavy Ni isotope signature (+1.64‰) is observed at the surface. The much higher Ni requirement of N_2 fixers than eukaryotic phytoplankton (Twining et al., 2012) leads to greater Ni surface removal at lower latitude stations, as confirmed by the particulate Ni export fluxes determined for GEOVIDE (averaging 49 µg/m^2/d at stations 13 and 21 compared to 14 µg/m^2/d at stations north of the SAF; Lemaitre et al., 2020). However, Station 21 in the west European basin is also characterised by a heavy Ni isotope signature (+1.67‰ at the surface), while cyanobacteria only represent 6% of the phytoplankton community (Tonnard, 2018). Here, nitrogen-fixing heterotrophic bacteria are abundant, as identified by *nifH* gene amplicon sequencing, which target the nitrogenase enzyme required for N_2 fixation (Fonseca-Batista et al., 2019). These non-cyanobacterial nitrogen fixers have recently been suggested to play a significant role in global N_2 fixation (Zehr and Capone, 2020). They could thus also be responsible for the high δ^{60}Ni value determined in surface waters of Station 21 (Fig. 4), as they likely have a high Ni requirement (Twining et al., 2012). Interestingly, these heterotrophic bacteria can also fix N_2 in the cold waters of the high latitude ocean (Blais et al., 2012), which may explain the moderately high N_2 fixation rate (D. Fonseca-Batista, personal communication, April 7, 2021) and the moderately elevated δ^{60}Ni value in the subpolar Irminger Sea (Station 44, N_2 fixation = 80 µmol N/m^2/d and δ^{60}Ni = +1.51‰ in surface; Fig. 4).

4.2. The high-low latitude biogeochemical divide

The new coupled Ni, NO_3^- isotope, and nitrogen fixation rate data from GEOVIDE (Figs. 3 and 4) indicate a link between surface Ni removal, Ni isotope fractionation and the presence of N_2 fixers. Though hypothesised previously (Archer et al., 2020; Middag et al., 2020; Yang et al., 2020), the lack of data from the same samples in the literature confines this direct comparison to GEOVIDE. To expand the latitudinal range of our analysis, we investigate the macronutrient/Ni/Ni isotope systematics of low versus high latitude waters of the Atlantic and Southern Ocean (Fig. 5).

A recent and comprehensive review of Ni concentration data for the Atlantic (Middag et al., 2020) highlighted the role of mixing of water masses in determining the Ni distribution, and the same simple process can explain the Ni-δ^{60}Ni arrays in our data compilation in Fig. 5. For example, all the deep ocean data are consistent with mixing between two end-members (end-members 1 and 2 on Fig. 5a and the solid black mixing curve) that have different Ni concentrations but rather similar δ^{60}Ni. The surface ocean at high latitudes also shows minimal Ni drawdown and isotope fractionation. However, a third end-member, at the lowest Ni concentrations and high δ^{60}Ni, is required to explain Ni and its isotopes in the upper low latitude ocean (dashed mixing curve; Fig. 5a). It is the generation of this end-member, via specific biogeochemical processes involving coupled Ni-N limitation in the low latitude surface ocean, that is our focus here.

The relationships between Ni, its isotopes, and the macronutrients are examined in Fig. 5b-d. The Ni concentration and $Si(OH)_4$ data for the deep low latitude ocean (Fig. 5b, open circles, >500 m) define an array, with invariant δ^{60}Ni, that again appears to be explained by mixing between the two deep ocean end-members. But the slopes of the Ni-$Si(OH)_4$ correlations are very different between the high latitude (all depths included, filled triangles) and upper 500 m low latitude (filled circles) regions. For all high latitude regions (black dashed lines in Fig. 5b), especially for the Southern Ocean, the arrays defined by the data for the upper ocean are less steep than those of the low latitude ocean (red dashed line in Fig. 5b). The very different Ni-$Si(OH)_4$ arrays have been noted before (Archer et al., 2020), and the particularly clear distinction between the upper depths of the low latitudes and the Southern Ocean is readily explained by the dominance

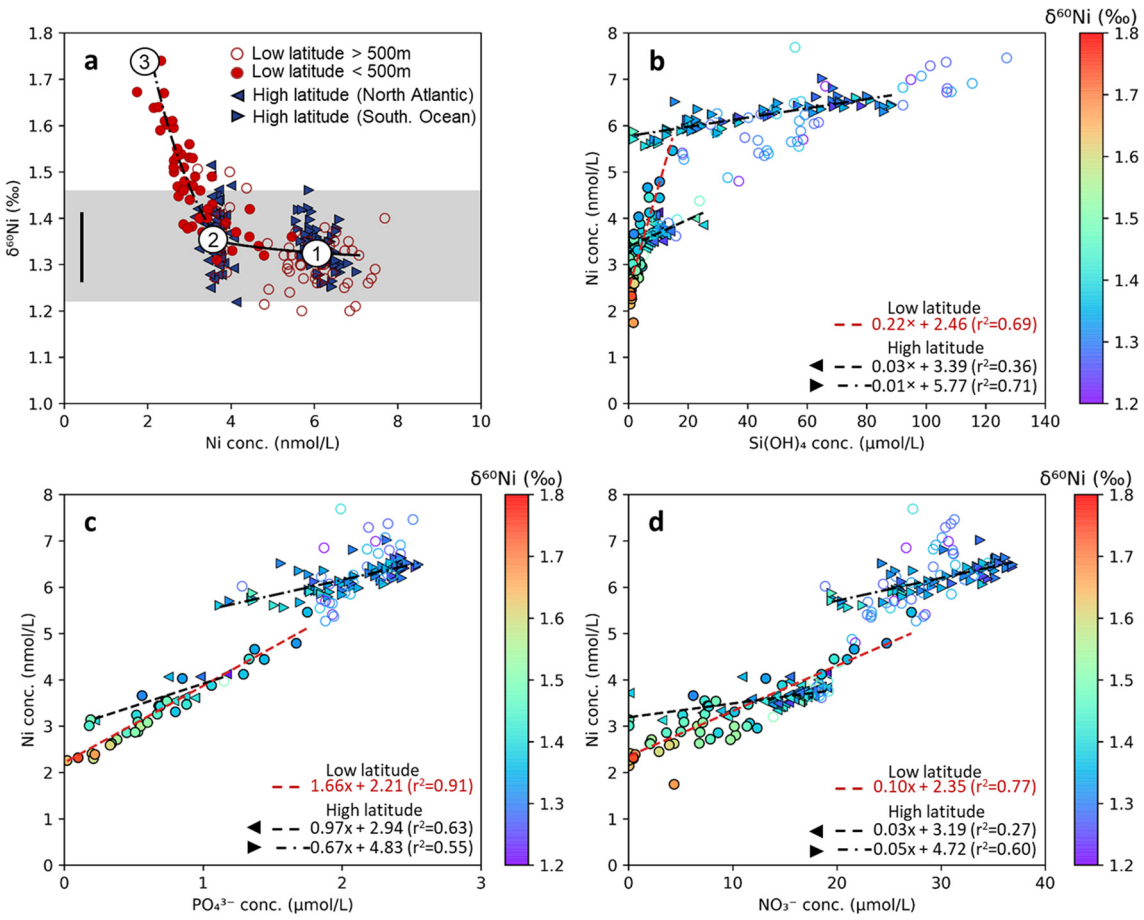

Fig. 5. Relationships between Ni, Ni isotopes and macronutrients in the Atlantic and Southern Ocean (Fig. S2). **a**) Dissolved Ni isotope composition versus Ni concentration. The grey bar shows the deep-ocean δ^{60}Ni value (see Fig. 2), the thick vertical black line shows the (2SD) reproducibility of Ni isotope measurements, and the black solid and dashed curves indicate mixing between putative end-members 1-3. End-member 3 represents the surface low latitude region; end-member 2 represents the subpolar North Atlantic region; and end-member 1 represents the Southern Ocean. Uptake of light isotopes, leaving heavy residual dissolved Ni (high δ^{60}Ni) in seawater, is very prominent in generating the Ni-poor low latitude surface ocean end-member (filled red circles), and creates a pattern of variation that contrasts strongly with both the Ni-rich low latitude deep ocean and the high latitudes at all depths. **b-d)** Ni-NO_3^--PO_4^{3-}-$Si(OH)_4$ systematics for samples for which isotope data are also available, colour-coded for Ni isotope compositions. As in **a**, empty symbols show low latitude data for depths > 500 m. The dashed lines highlight the contrasting pattern of covariation between Ni and the macro-nutrients in low versus high latitude regions of the upper ocean (<500 m). The two different high latitude groups are from the Southern Ocean ([Ni] > 5 nmol/L) and the North Atlantic (3 > [Ni] > 4.5 nmol/L). Similar systematics are also observed for GEOTRACES IDP2021 data for the entire Atlantic Ocean (see Fig. S6). (For interpretation of the colours in the figure(s), the reader is referred to the web version of this article.)

of diatoms in the phytoplankton ecology of the latter, which strip $Si(OH)_4$ from surface waters and release it at depth after remineralisation, but appear to only marginally alter Ni concentrations and isotopes (Wang et al., 2019). Although Twining et al. (2012) emphasise that diatoms are enriched in Ni, with 50% of cellular Ni found in the frustule, the authors also suggest that nitrogen-fixing cyanobacteria have greater Ni requirements and are characterised by the highest cellular Ni/P ratios. Figs. 5c, d extend this treatment to NO_3^- and PO_4^{3-}, where the separation between the high and low latitude surface oceans is less pronounced but still evident in different slopes. These different systematics are also observed for concentration data from the entire Atlantic Ocean (Fig. S6; GEOTRACES Intermediate Data Product, 2021), and emphasise once again the biogeochemical divide between the low and the high latitude oceans (Sarmiento et al., 2004; Vance et al., 2017).

It is notable that, for all Ni-macronutrient relationships, the most fractionated Ni isotope compositions lie at the low-Ni end of the low latitude data arrays in Figs. 5b-d, implying that the isotopically fractionated end-member 3 in Fig. 5a is coupled to distinct Ni/macronutrient ratios. The data arrays that link end-member 3 to the sub-thermocline ocean are produced by a complex interaction between low latitude uptake (with isotope fractionation) and ocean circulation. Nonetheless, it is clear that this end-member must be generated via the peculiar biogeochemistry of the low latitude surface ocean that reduces Ni concentrations more strongly, relative to the macronutrients, than high-latitude uptake. It is also noteworthy that the difference in the slopes of the data arrays in Fig. 5b-d mirror the difference in Ni/macronutrient uptake ratios reported for the key phytoplankton in these ocean regions. For example, the average Ni/PO_4 and Ni/$Si(OH)_4$ slopes for the high latitude ocean (0.82 mmol/mol and 0.02 mmol/mol respectively; Fig. 5) are similar to Ni/P and Ni/Si found in the diatoms that are known to dominate the phytoplankton community in high latitude regions (0.52 mmol/mol and 0.03 mmol/mol, respectively; Twining et al., 2012). Conversely, the much higher Ni/PO_4 and Ni/$Si(OH)_4$ slopes for the low latitude upper ocean, with values reaching 1.66 and 0.22 mmol/mol, respectively, are higher than for diatoms, and the Ni/P ratios is much closer to those observed for cyanobacteria (up to 3.40 mmol/mol; Dupont et al., 2010; Twining et al., 2012).

4.3. Large-scale controls on the marine Ni cycle

Our new data (Section 4.1) and the analysis of the basin-scale distribution of Ni (Section 4.2) suggest that low-latitude Ni utilisation and associated fractionation are the main drivers of the marine Ni and δ^{60}Ni distributions. Previous studies have attempted

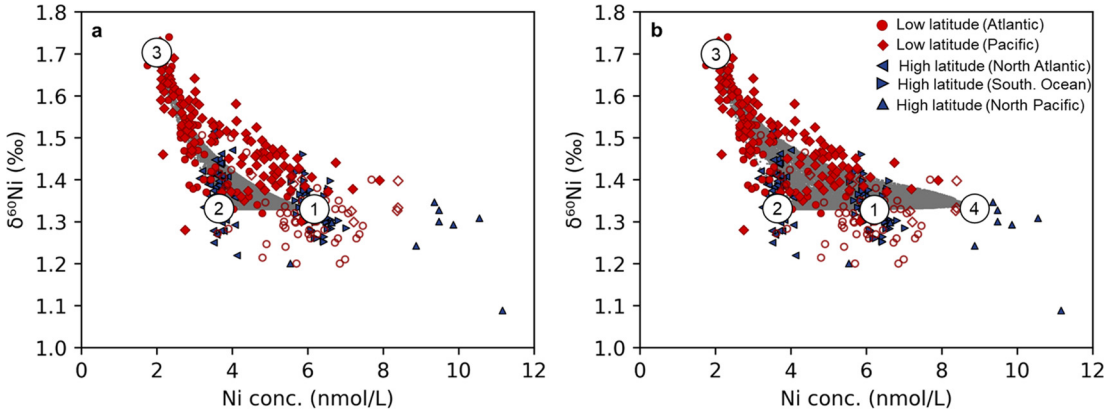

Fig. 6. Comparison of the dissolved Ni-δ^{60}Ni systematics observed in the world ocean (in colours) with the results of the Total Matrix Intercomparison model (in grey) when simulating a) only physical propagation of surface properties into the interior; b) physical circulation and remineralisation of Ni with δ^{60}Ni = +1.33‰ at both high and low latitudes. Empty symbols illustrate depths > 500 m in low latitude regions. End-members 1, 2, 3 are described in the caption to Fig. 5 and end-member 4 represents the North Pacific. A test of the sensitivity of model results to the δ^{60}Ni value of low-latitude remineralisation is presented in Fig. S3. Locations and citations for data from the literature are given in Fig. S2. (For interpretation of the colours in the figure(s), the reader is referred to the web version of this article.)

to separate the influence of physical circulation and biological cycling in determining marine Ni-δ^{60}Ni systematics based on limited regional datasets (Archer et al., 2020; Yang et al., 2021). Here, we go further and use the observationally constrained TMI (Section 2.3) to perform mixing calculations on the global scale (Gebbie and Huybers, 2010), incorporating oceanographic information on water-mass mixing, and examine its impact on the oceanic distributions of Ni and its isotopes. We further add a biological component by linking Ni to PO_4^{3-} cycling. Because the surface ocean is treated as a boundary condition in TMI, we cannot investigate the *cause* of the distribution of surface ocean Ni-δ^{60}Ni, in particular the heavy δ^{60}Ni of the low latitude surface (Archer et al., 2020; Yang et al., 2021). The purpose of this modelling effort is not to derive model parameters by finding a "best fit" to the observations, but rather to investigate the degree to which most of the global variations in the data can be explained by just a few major processes, including ocean circulation, the production of a fractionated, Ni-poor reservoir in the low-latitude surface, and interior regeneration of Ni. A fully prognostic ocean biogeochemical model is needed to study the global Ni cycle in its complete form in the future. Our preliminary modelling study here helps to elucidate the most important global processes, that should be studied in detail using more comprehensive models.

A model that only propagates surface boundary conditions through physical circulation reasonably captures the distributions of Ni-δ^{60}Ni in the Atlantic and Southern Ocean but not in the Pacific (Fig. 6a). This is because the vigorous Atlantic and Southern Ocean circulation exerts a dominant control on macro- and micro-nutrient distributions over biological cycling (Middag et al., 2020). On the contrary, the sluggish circulation in the Pacific allows the influence of remineralisation to manifest more clearly. Indeed, adding a remineralised component allows the model to better reproduce the high Ni concentrations in the deep Pacific (Fig. 6b), while also improving the fit to Ni concentrations at intermediate depths of the low latitude Atlantic Ocean (Fig. 2a). Furthermore, the remineralised δ^{60}Ni in low latitude regions needs to be close to +1.3‰ to produce global Ni-δ^{60}Ni systematics (Fig. S3), in agreement with particulate observations (Yang et al., 2021).

Thus, in agreement with our data-based analysis in Section 4.3, our model - despite its simplicity - shows that the main features of the global Ni-δ^{60}Ni systematics can be explained by the interaction between physical circulation, production of a high-δ^{60}Ni low-latitude surface end-member, and the regeneration of a complementary low δ^{60}Ni signal in the ocean interior. In contrast to Yang et al. (2021), who invoke the addition of isotopically heavy Ni to deep waters in order to explain the global marine Ni-δ^{60}Ni systematics, we find that the difference in Ni-δ^{60}Ni systematics between the Atlantic and Pacific Oceans visible in Fig. 6 is fully consistent with our limited set of model processes: even in the presence of an isotopically uniform deep ocean as simulated by our model, the elevated concentrations of Ni in the Pacific result in a distinct Ni-δ^{60}Ni trajectory in the upper ocean sampled by Yang et al. (2021). Our model results thus suggest that extending observational coverage to the deep Pacific will reveal no significant δ^{60}Ni difference between Pacific and Atlantic deep waters.

4.4. Potential origins of the heavy surface end-member

Corroborating the inferences from our North Atlantic data, the basin-scale δ^{60}Ni systematics and Ni-macronutrient relationships suggest a unique isotopically fractionated, Ni-poor end-member in the low latitude surface ocean. Culturing experiments have demonstrated that elevated phytoplankton Ni requirements result from the importance of three different Ni-containing enzymes that are key to the physiology of prokaryotes in the oligotrophic low latitude ocean. The enzyme urease, which converts urea into ammonium, enables N acquisition where dissolved inorganic nitrogen is not available (McCarthy, 1972), i.e. in most of the low latitude surface ocean (Moore et al., 2013). The enzyme SOD is essential for aerobic organisms (Ragsdale, 2009), with Ni-SOD the only isoform found in some ubiquitous low latitude cyanobacteria and some heterotrophic bacteria (Dupont et al., 2008b). Finally, the enzyme Ni-Fe hydrogenase, found in heterotrophic bacteria and cyanobacteria (Barz et al., 2010), is involved in biological hydrogen turnover (Ragsdale, 2009). Both Ni-SOD and Ni-Fe hydrogenase have been shown to promote optimal rates of N_2 fixation (Rodriguez and Ho, 2014). These enzymatic links between the Ni and N cycles clearly imply a bioactive role of Ni in the ocean.

The bioactive role of Ni is likely reinforced in the warm oligotrophic waters of the low latitude ocean. Here, cyanobacteria are the dominant photosynthesisers (Partensky and Garczarek, 2010), the lack of fixed inorganic nitrogen leads to greater urease activity and creates a niche for diazotrophs, and high light conditions increase the concentration of superoxide species. But, because of these different roles of Ni in different aspects of nitrogen metabolism in different organisms, we cannot at this stage definitively establish which specific process, or combination of processes, in the nitrogen cycle is mechanistically coupled to Ni depletion and isotope fractionation. What is clear is that the prokaryote-dominated low latitude ocean sees substantially greater Ni drawdown relative to macronutrients, while the eukaryote-dominated

high latitudes do not. In this view, the surface low latitude ocean, which is also highly depleted in inorganic N, may be Ni-N co-limited.

In the south Atlantic, Archer et al. (2020) suggested that seawater Ni-δ^{60}Ni systematics are not consistent with the entire dissolved pool of Ni being bio-available. Instead, these authors suggest that the data can only be explained by near-total exhaustion of the bio-available pool at total dissolved Ni concentrations around 1.7 nmol/L. The low δ^{60}Ni of regenerated Ni (+1.2 to +1.4‰) simulated in our model is consistent both with bio-availability of the entire Ni pool, and with a partitioning of dissolved Ni between an isotopically lighter bio-available pool (+1.2‰) and an isotopically heavier organically complexed pool that is inaccessible to biology (+1.7‰; Archer et al., 2020). Although many lines of evidence suggest that a large portion of the low latitude surface ocean Ni pool is not bio-available (Price and Morel, 1991; Mackey et al., 2002; Wen et al., 2006; Egleston and Morel, 2008; Dupont et al., 2008a, 2010; Ho, 2013), at this stage and without prognostic model simulations with explicit representations of surface-ocean fractionation, we cannot differentiate between these two hypotheses.

5. Summary, conclusions and outlook

In this study, we have presented new Ni concentrations and isotope compositions from the GEOVIDE transect in the North Atlantic. Depth profiles of Ni isotopes display a homogeneous deep ocean signature. This homogeneity extends to the entire water column at stations north of the Subarctic Front, but significantly higher δ^{60}Ni is observed in the surface waters of the low latitude stations. The comparison of our new Ni data to NO_3^- isotopes and N_2 fixation rates, also determined during GEOVIDE, strongly suggests a link between N_2 fixation and Ni isotope fractionation in the surface waters of these low latitude stations (Fonseca-Batista et al., 2019; Deman et al., 2021; D. Fonseca-Batista, personal communication, April 7, 2021). Combining our data with the growing open-ocean Ni isotope database, data analysis and a simple global Ni cycling model show that Ni-macronutrient and Ni-δ^{60}Ni systematics require the creation of a high-δ^{60}Ni, Ni-poor end-member in the low latitudes, consistent with higher Ni requirements in these waters dominated by prokaryotes compared to eukaryote-dominated high latitude regions. It appears that the peculiar Ni biogeochemistry in the low latitudes arises from some combination of the three different Ni-bearing enzymes that are important for the physiology of prokaryotes. Therefore, we suggest that the surface low latitude ocean, which is also highly depleted in inorganic N, may be Ni-N co-limited, in agreement with culturing and recent Ni isotope studies.

The analysis here has been limited to the modern ocean. However, the very strong correlations between Ni concentrations and organic carbon in organic-rich marine sediments, perhaps the strongest of any transition metal (Algeo and Maynard, 2004; Böning et al., 2015; Ciscato et al., 2018), suggest a key long-term bioactive role for Ni, which would prove a highly fruitful future research direction. Our new findings suggest that more detailed experimental studies of this neglected metal will be key in determining the precise biogeochemical role of Ni: both culturing studies to investigate intra-cellular quotas and their relation to the activity of Ni-SOD and NiFe-hydrogenase, as well as incubation experiments in appropriate areas of the low-latitude ocean.

CRediT authorship contribution statement

Nolwenn Lemaitre, Corey Archer and Derek Vance conceived the study. Nolwenn Lemaitre and Derek Vance wrote the first draft of the paper. Jianghui Du and Gregory F. de Souza constrained the Nimacronutrient systematics and the three-dimensional model of Ni cycling. All authors read, commented and helped to refine the interpretation of the paper.

Declaration of competing interest

The authors declare that they have no known competing financial interests or personal relationships that could have appeared to influence the work reported in this paper.

Acknowledgements

Special thanks go to Hélène Planquette and Géraldine Sarthou (Géraldine Sarthou also as co-chief scientist) for leading the clean trace metal sampling during the GEOVIDE cruise, as well as to all members of the sampling team including Julia Boutorh, Marie Cheize, Leonardo Contreira Pereira, François Lacan, Jan-Lukas Menzel Barraqueta and Rachel Shelley. We would like to thank the captain, the crew and the co-chief scientist Pascale Lherminier, for their great work and support during the GEOVIDE cruise. We also would like to thank Fabien Perault and Emmanuel De Saint Léger (CNRS DT-INSU) for their help during the CTD deployments; Catherine Schmechtig for the GEOVIDE database management; Emilie Grossteffan, Manon Le Goff, Morgane Gallinari and Paul Tréguer (LEMAR, IUEM) for the analysis of nutrients. Finally, we thank the two reviewers and the editor for comments that helped to improve this manuscript. The GEOVIDE project was supported by the French National Research Agency (ANR-13-BS06-0014 and ANR-12-PDOC-0025-01), the French National Centre for Scientific Research (CNRS-LEFE-CYBER), Ifremer and the "Laboratoire d'Excellence" Labex-Mer (ANR-10-LABX-19). This work received financial support from the Swiss National Science Foundation through grant 200020_165904. This project has received funding from the European Union's Horizon 2020 research and innovation programme under the Marie Skłodowska-Curie grant agreement 891489.

Appendix A. Supplementary material

Supplementary material related to this article can be found online at https://doi.org/10.1016/j.epsl.2022.117513.

References

Algeo, T.J., Maynard, J.B., 2004. Trace-element behavior and redox facies in core shales of upper Pennsylvanian Kansas-type cyclothems. Chem. Geol. 206, 289–318. https://doi.org/10.1016/j.chemgeo.2003.12.009.

Archer, C., Vance, D., Milne, A., Lohan, M.C., 2020. The oceanic biogeochemistry of nickel and its isotopes: new data from the South Atlantic and the Southern Ocean biogeochemical divide. Earth Planet. Sci. Lett. 535, 116118. https://doi.org/10.1016/j.epsl.2020.116118.

Barz, M., Beimgraben, C., Staller, T., Germer, F., Opitz, F., Marquardt, C., Schwarz, C., Gutekunst, K., Vanselow, K.H., Schmitz, R., LaRoche, J., Schulz, R., Appel, J., 2010. Distribution analysis of hydrogenases in surface waters of marine and freshwater environments. PLoS ONE 5, e13846. https://doi.org/10.1371/journal.pone.0013846.

Blais, M., Tremblay, J.É., Jungblut, A.D., Gagnon, J., Martin, J., Thaler, M., Lovejoy, C., 2012. Nitrogen fixation and identification of potential diazotrophs in the Canadian Arctic. Glob. Biogeochem. Cycles 26, 1–13. https://doi.org/10.1029/2011GB004096.

Böning, P., Shaw, T., Pahnke, K., Brumsack, H.-J., 2015. Nickel as indicator of fresh organic matter in upwelling sediments. Geochim. Cosmochim. Acta 162, 99–108. https://doi.org/10.1016/j.gca.2015.04.027.

Bonnet, S., Caffin, M., Berthelot, H., Moutin, T., 2017. Hot spot of N2 fixation in the western tropical South Pacific pleads for a spatial decoupling between N2 fixation and denitrification. Proc. Natl. Acad. Sci. 114, 2800–2801. https://doi.org/10.1073/pnas.1619514114.

Bruland, K.W., 1980. Oceanographic distributions of cadmium, zinc, nickel, and copper in the North Pacific. Earth Planet. Sci. Lett. 47, 176–198. https://doi.org/10.1016/0012-821X(80)90035-7.

Bruland, K.W., Middag, R., Lohan, M.C., 2014. Controls of trace metals in seawater. In: Holland, H.D., Turekian, K.K. (Eds.), Treatise on Geochemistry, second edition. Elsevier Ltd., pp. 19–51.

Caffin, M., Moutin, T., Foster, R.A., Bouruet-Aubertot, P., Doglioli, A.M., Berthelot, H., Guieu, C., Grosso, O., Helias-Nunige, S., Leblond, N., Gimenez, A., Petrenko, A.A., de Verneil, A., Bonnet, S., 2018. N2 fixation as a dominant new N source in the western tropical South Pacific Ocean (OUTPACE cruise). Biogeosciences 15, 2565–2585. https://doi.org/10.5194/bg-15-2565-2018.

Cameron, V., Vance, D., 2014. Heavy nickel isotope compositions in rivers and the oceans. Geochim. Cosmochim. Acta 128, 195–211. https://doi.org/10.1016/j.gca.2013.12.007.

Capone, D.G., Burns, J.A., Montoya, J.P., Subramaniam, A., Mahaffey, C., Gunderson, T., Michaels, A.F., Carpenter, E.J., 2005. Nitrogen fixation by Trichodesmium spp.: an important source of new nitrogen to the tropical and subtropical North Atlantic Ocean. Glob. Biogeochem. Cycles 19, 1–17. https://doi.org/10.1029/2004GB002331.

Ciscato, E.R., Bontognali, T.R.R., Vance, D., 2018. Nickel and its isotopes in organic-rich sediments: implications for oceanic budgets and a potential record of ancient seawater. Earth Planet. Sci. Lett. 494, 239–250. https://doi.org/10.1016/j.epsl.2018.04.061.

Cutter, G., Casciotti, K., Croot, P., Geibert, W., Heimbürger, L.-E., Lohan, M., Planquette, H., Van De Flierdt, T., 2017. Sampling and the sample-handling protocoles for GEOTRACES cruises. http://www.geotraces.org/science/intercalibration/222-sampling-and-sample-handling-protocols-for-geotraces-cruises.

Deman, F., Fonseca-Batista, D., Roukaerts, A., García-Ibáñez, M.I., Le Roy, E., Thilakarathne, E.P.D.N., Elskens, M., Dehairs, F., Fripiat, F., 2021. Nitrate supply routes and impact of internal cycling in the North Atlantic Ocean inferred from nitrate isotopic composition. Glob. Biogeochem. Cycles 35, e2020GB006887. https://doi.org/10.1029/2020GB006887.

Dickson, R.R., Brown, J., 1994. The production of North Atlantic deep water: sources, rates, and pathways. J. Geophys. Res. 99, 12319–12341. https://doi.org/10.1029/94JC00530.

Dupont, C.L., Barbeau, K., Palenik, B., 2008a. Ni uptake and limitation in marine synechococcus strains. Appl. Environ. Microbiol. 74, 23–31. https://doi.org/10.1128/AEM.01007-07.

Dupont, C.L., Buck, K.N., Palenik, B., Barbeau, K., 2010. Nickel utilization in phytoplankton assemblages from contrasting oceanic regimes. Deep-Sea Res., Part 1, Oceanogr. Res. Pap. 57, 553–566. https://doi.org/10.1016/j.dsr.2009.12.014.

Dupont, C.L., Neupane, K., Shearer, J., Palenik, B., 2008b. Diversity, function and evolution of genes coding for putative Ni-containing superoxide dismutases. Environ. Microbiol. 10, 1831–1843. https://doi.org/10.1111/j.1462-2920.2008.01604.x.

Egleston, E.S., Morel, M.M., 2008. Nickel limitation and zinc toxicity in a urea-grown diatom. Limnol. Oceanogr. 53, 2462–2471. https://doi.org/10.4319/lo.2008.53.6.2462.

Fonseca-Batista, D., Li, X., Riou, V., Michotey, V., Deman, F., Fripiat, F., Guasco, S., Brion, N., Lemaitre, N., Tonnard, M., Gallinari, M., Planquette, H., Planchon, F., Sarthou, G., Elskens, M., LaRoche, J., Chou, L., Dehairs, F., 2019. Evidence of high N2 fixation rates in the temperate northeast Atlantic. Biogeosciences 16, 999–1017. https://doi.org/10.5194/bg-16-999-2019.

García-Ibáñez, M.I., Pérez, F.F., Lherminier, P., Zunino, P., Mercier, H., Tréguer, P., 2018. Water mass distributions and transports for the 2014 GEOVIDE cruise in the North Atlantic. Biogeosciences 15, 2075–2090. https://doi.org/10.5194/bg-15-2075-2018.

Garcia, H., Weathers, K., Paver, C., Smolyar, I., Boyer, T., Locarnini, M., Zweng, M., Mishonov, A., Baranova, O., Seidov, D., Reagan, J., 2019. World Ocean Atlas 2018. Vol. 4: Dissolved Inorganic Nutrients (Phosphate, Nitrate and Nitrate+Nitrite, Silicate).

Gebbie, G., Huybers, P., 2010. Total matrix intercomparison: a method for determining the geometry of water-mass pathways. J. Phys. Oceanogr. 40, 1710–1728. https://doi.org/10.1175/2010JPO4272.1.

GEOTRACES Intermediate Data Product Group, 2021. The GEOTRACES Intermediate Data Product 2021 (IDP2021). NERC EDS Br. Oceanogr. Data Cent. NOC.

Gourain, A., Planquette, H., Cheize, M., Lemaitre, N., Menzel Barraqueta, J.L., Shelley, R., Lherminier, P., Planquette, H., 2019. Inputs and processes affecting the distribution of particulate iron in the North Atlantic along the GEOVIDE (GEOTRACES GA01) section. Biogeosciences 16, 1563–1582. https://doi.org/10.5194/bg-16-1563-2019.

Gradoville, M.R., Farnelid, H., White, A.E., Turk-kubo, K.A., Stewart, B., Ribalet, F., Ferrón, S., Pinedo-gonzalez, P., Armbrust, E.V., Karl, D.M., John, S., Zehr, J.P., 2020. Latitudinal constraints on the abundance and activity of the cyanobacterium UCYN-A and other marine diazotrophs in the North Pacific. Limnol. Oceanogr. 65, 1858–1875. https://doi.org/10.1002/lno.11423.

Gueguen, B., Rouxel, O., 2021. The Nickel isotope composition of the authigenic sink and the diagenetic flux in modern oceans. Chem. Geol. 563, 120050. https://doi.org/10.1016/j.chemgeo.2020.120050.

Gueguen, B., Rouxel, O., Ponzevera, E., Bekker, A., Fouquet, Y., 2013. Nickel isotope variations in terrestrial silicate rocks and geological reference materials measured by MC-ICP-MS. Geostand. Geoanal. Res. 37, 297–317. https://doi.org/10.1111/j.1751-908X.2013.00209.x.

Ho, T., 2013. Nickel limitation of nitrogen fixation in Trichodesmium. Limnol. Oceanogr. 58, 112–120. https://doi.org/10.4319/lo.2013.58.1.0112.

Ho, T., Chu, T., Hu, C., 2013. Interrelated influence of light and Ni on Trichodesmium growth. Front. Microbiol. 4, 1–6. https://doi.org/10.3389/fmicb.2013.00139.

Karstensen, J., Tomczak, M., 1998. Age determination of mixed water masses using CFC and oxygen data. J. Geophys. Res. 103, 18599–18609.

Konhauser, K.O., Pecoits, E., Lalonde, S.V., Papineau, D., Nisbet, E.G., Barley, M.E., Arndt, N.T., Zahnle, K., Kamber, B.S., 2009. Oceanic nickel depletion and a methanogen famine before the great oxidation event. Nature 458, 750–753. https://doi.org/10.1038/nature07858.

Lemaitre, N., Planquette, H., Dehairs, F., Planchon, F., Sarthou, G., Gallinari, M., Roig, S., Jeandel, C., Castrillejo, M., 2020. Particulate trace element export in the North Atlantic (GEOTRACES GA01 transect, GEOVIDE cruise). ACS Earth Space Chem. 4, 2185–2204. https://doi.org/10.1021/acsearthspacechem.0c00045.

Little, S.H., Archer, C., McManus, J., Najorka, J., Wegorzewski, A.V., Vance, D., 2020. Towards balancing the oceanic Ni budget. Earth Planet. Sci. Lett. 547, 116461. https://doi.org/10.1016/j.epsl.2020.116461.

Luo, Y.W., Doney, S.C., Anderson, L.A., Benavides, M., Bode, A., Bonnet, S., Capone, D.G., Carpenter, E.J., Chen, Y.L., Church, M.J., Dore, J.E., Foster, R.A., Furuya, K., Gundersen, K., Hynes, A.M., Karl, D.M., Kitajima, S., Langlois, R.J., Laroche, J., Letelier, R.M., Moisander, P.H., Moore, C.M., Mulholland, M.R., Needoba, J.A., Orcutt, K.M., Poulton, A.J., Rahav, E., Raimbault, P., Rees, A.P., Riemann, L., Shiozaki, T., Subramaniam, A., Tyrrell, T., Varela, M., Villareal, T.A., Webb, E.A., White, A.E., Wu, J., Zehr, J.P., 2012. Database of diazotrophs in global ocean: abundance, biomass and nitrogen fixation rates. Earth Syst. Sci. Data 4, 47–73. https://doi.org/10.5194/essd-4-47-2012.

Mackey, D.J., O'Sullivan, J.E., Watson, R.J., Dal Pont, G., 2002. Trace metals in the Western Pacific: temporal and spatial variability in the concentrations of Cd, Cu, Mn and Ni. Deep-Sea Res., Part 1, Oceanogr. Res. Pap. 49, 2241–2259. https://doi.org/10.1016/S0967-0637(02)00124-3.

McCarthy, J.J., 1972. The uptake of urea by natural populations of marine phytoplankton. Limnol. Oceanogr. 17, 738–748. https://doi.org/10.4319/lo.1972.17.5.0738.

Middag, R., De Baar, H.J.W., Bruland, K.W., van Heuven, S.M.A.C., 2020. The distribution of nickel in the West-Atlantic Ocean, its relationship with phosphate and a comparison to cadmium and zinc. Front. Mar. Sci. 7, 1–17. https://doi.org/10.3389/fmars.2020.00105.

Moore, C.M., Mills, M.M., Arrigo, K.R., Berman-Frank, I., Bopp, L., Boyd, P.W., Galbraith, E.D., Geider, R.J., Guieu, C., Jaccard, S.L., Jickells, T.D., La Roche, J., Lenton, T.M., Mahowald, N.M., Maranon, E., Marinov, I., Moore, J.K., Nakatsuka, T., Oschlies, A., Saito, M.A., Thingstad, T.F., Tsuda, A., Ulloa, O., 2013. Processes and patterns of oceanic nutrient limitation. Nat. Geosci. 6, 701–710. https://doi.org/10.1038/ngeo1765.

Partensky, F., Garczarek, L., 2010. Prochlorococcus: advantages and limits of minimalism. Annu. Rev. Mar. Sci. 2, 305–331. https://doi.org/10.1146/annurev-marine-120308-081034.

Price, N.M., Morel, F.M.M., 1991. Colimitation of phytoplankton growth by nickel and nitrogen. Limnol. Oceanogr. 36, 1071–1077. https://doi.org/10.4319/lo.1991.36.6.1071.

Ragsdale, S.W., 2009. Nickel-based enzyme systems. J. Biol. Chem. 284, 18571–18575. https://doi.org/10.1074/jbc.R900020200.

Raven, J.A., 1998. The twelfth Tansley lecture. Small is beautiful: the picophytoplankton. Funct. Ecol. 12, 503–513. https://doi.org/10.1046/j.1365-2435.1998.00233.x.

Rodriguez, I.B., Ho, T.Y., 2014. Diel nitrogen fixation pattern of Trichodesmium: the interactive control of light and Ni. Sci. Rep. 4, 1–5. https://doi.org/10.1038/srep04445.

Sarmiento, J.L., Gruber, N., Brzezinski, M.A., Dunne, J.P., 2004. High-latitude controls of thermocline nutrients and low latitude biological productivity. Nature 427, 56–60. https://doi.org/10.1038/nature10605.

Sclater, F.R., Boyle, E., Edmond, J.M., 1976. On the marine geochemistry of nickel. Earth Planet. Sci. Lett. 31, 119–128. https://doi.org/10.1016/0012-821X(76)90103-5.

Selden, C.R., Mulholland, M.R., Bernhardt, P.W., Widner, B., Macías-Tapia, A., Ji, Q., Jayakumar, A., 2019. Dinitrogen fixation across physico - chemical gradients of the Eastern Tropical North Pacific Oxygen deficient zone global biogeochemical cycles. Glob. Planet. Change 33, 1187–1202. https://doi.org/10.1029/2019GB006242.

Sohrin, Y., Urushihara, S., Nakatsuka, S., Kono, T., Higo, E., Minami, T., Norisuye, K., Umetani, S., 2008. Multielemental determination of GEOTRACES key trace metals in seawater by ICPMS after preconcentration using an ethylenediaminetriacetic acid chelating resin. Anal. Chem. 80, 6267–6273. https://doi.org/10.1021/ac800500f.

Sun, M., Archer, C., Vance, D., 2021. New methods for the chemical isolation and stable isotope measurement of multiple transition metals, with application to the Earth sciences. Geostand. Geoanal. Res., 1–16. https://doi.org/10.1111/ggr.12402.

Takano, S., Tanimizu, M., Hirata, T., Shin, K.-C., Fukami, Y., Suzuki, K., Sohrin, Y., 2017. A simple and rapid method for isotopic analysis of nickel, copper, and zinc in seawater using chelating extraction and anion exchange. Anal. Chim. Acta 967, 1–11. https://doi.org/10.1016/j.aca.2017.03.010.

Tang, W., Li, Z., Cassar, N., 2019. Machine learning estimates of global marine nitrogen fixation. J. Geophys. Res., Biogeosci. 124, 717–730. https://doi.org/10.1029/2018JG004828.

Tonnard, M., 2018. Etude du cycle biogéochimique du fer: Distribution et spéciation dans l'océan Atlantique nord (GA01) et l'océan Austral (GIpr05) (GEOTRACES). Université de Bretagne Occidentale & Université de Tasmanie.

Twining, B.S., Baines, S.B., Vogt, S., Nelson, D.M., 2012. Role of diatoms in nickel biogeochemistry in the ocean. Glob. Biogeochem. Cycles 26, 1–9. https://doi.org/10.1029/2011GB004233.

Vance, D., Little, S.H., Archer, C., Cameron, V., Andersen, M.B., Rijkenberg, M.J.A., Lyons, T.W., 2016. The oceanic budgets of nickel and zinc isotopes: the importance of sulfidic environments as illustrated by the Black Sea. Philos. Trans. R. Soc. Lond. A 374. https://doi.org/10.1098/rsta.2015.0294.

Vance, D., Little, S.H., de Souza, G.F., Khatiwala, S., Lohan, M.C., Middag, R., 2017. Silicon and zinc biogeochemical cycles coupled through the Southern Ocean. Nat. Geosci., 1–6. https://doi.org/10.1038/ngeo2890.

Wang, R.M., Archer, C., Bowie, A.R., Vance, D., 2019. Zinc and nickel isotopes in seawater from the Indian sector of the Southern Ocean: the impact of natural iron fertilization versus Southern Ocean hydrography and biogeochemistry. Chem. Geol. 511, 452–464. https://doi.org/10.1016/j.chemgeo.2018.09.010.

Watt, R.K., Ludden, P.W., 1999. Nickel-binding proteins. Cell. Mol. Life Sci. 56, 604–625. https://doi.org/10.1007/s000180050456.

Wen, L.S., Jiann, K.T., Santschi, P.H., 2006. Physicochemical speciation of bioactive trace metals (Cd, Cu, Fe, Ni) in the oligotrophic South China Sea. Mar. Chem. 101, 104–129. https://doi.org/10.1016/j.marchem.2006.01.005.

Yang, S., Kelly, R.L., Bian, X., Conway, T.M., Huang, K., Ho, T., Neibauer, J.A., Keil, R.G., Moffett, J.W., John, S.G., 2021. Lack of redox cycling for nickel in the water column of the eastern tropical North Pacific oxygen deficient zone: insight from dissolved and particulate nickel isotopes. Geochim. Cosmochim. Acta 309, 235–250. https://doi.org/10.1016/j.gca.2021.07.004.

Yang, S.C., Hawco, N.J., Pinedo-González, P., Bian, X., Huang, K.-F., Zhang, R., John, S.G., 2020. A new purification method for Ni and Cu stable isotopes in seawater provides evidence for widespread Ni isotope fractionation by phytoplankton in the North Pacific. Chem. Geol. 547, 119662. https://doi.org/10.1016/j.chemgeo.2020.119662.

Zehr, J.P., Capone, D.G., 2020. Changing perspectives in marine nitrogen fixation. Science 80, 368. https://doi.org/10.1126/science.aay9514.

Zunino, P., Lherminier, P., Mercier, H., Daniault, N., García-Ibáñez, M.I., Pérez, F.F., 2017. The GEOVIDE cruise in May-June 2014 reveals an intense meridional overturning circulation over a cold and fresh subpolar North Atlantic. Biogeosciences 14, 5323–5342. https://doi.org/10.5194/bg-14-5323-2017.